

Surface atomic configurations due to dislocation activity in InAs/GaAs(110) heteroepitaxy

J. G. Belk

*Semiconductor Materials IRC, Imperial College, London SW7 2BZ, United Kingdom
and Department of Chemistry, Imperial College, London, SW7 2AY, United Kingdom*

D. W. Pashley

Department of Materials, Imperial College, London, SW7 2BP, United Kingdom

C. F. McConville*

*Semiconductor Materials IRC, Imperial College, London SW7 2BZ, United Kingdom
and Department of Chemistry, Imperial College, London, SW7 2AY, United Kingdom*

J. L. Sudijono[†] and B. A. Joyce

Semiconductor Materials IRC, Imperial College, London SW7 2BZ, United Kingdom

T. S. Jones[‡]

*Semiconductor Materials IRC, Imperial College, London SW7 2BZ, United Kingdom
and Department of Chemistry, Imperial College, London, SW7 2AY, United Kingdom*

(Received 5 May 1997)

The surface of a compressively strained InAs epilayer grown on a GaAs(110) substrate has been resolved at the atomic level by scanning tunneling microscopy. The growth of the InAs film (>5 ML) involves a class of dislocations which are nucleated at the surface and subsequently channeled down to relieve the strain at the buried interface with the GaAs substrate. The effects of the disruption to the atomic geometry in the InAs surface layer due to this dislocation motion, and the accommodation of these imperfections by continuing epitaxy, are presented. [S0163-1829(97)09839-1]

I. INTRODUCTION

One of the most well-known types of misfit dislocation in covalent epitaxial layers with the sphalerite or face-centered-cubic crystal structure lies on the $\{111\}$ slip planes between the epilayer surface and the substrate interface.¹ The dislocation line is approximately half-looped in shape, possessing a straight interfacial misfit segment enclosed by two threading segments which extend to the surface, varying in character from screw to edge and back to screw-type along its length. In the case of growth on the (110) surface, it is the (111) and $(11\bar{1})$ planes that are inclined at 35.3° to (110) which contain these dislocations, accounting for uniaxial strain relief in the $[001]$ direction in the layer.²

Strain relief for the compound semiconductor growth system, InAs/GaAs(110), is anisotropic and occurs via two separate pathways. The $\{111\}$ slip plane dislocations are preceded in thickness terms by the direct nucleation of pure edge-type dislocations to achieve the necessary biaxial relaxation.³ Both types of dislocation can be distinguished by scanning tunneling microscopy (STM), although the imaging mechanism in each case is different.^{4,5} In a previous paper, we focused on the set of edge dislocations which produce a sub-Å undulation in the atomic planes along $[001]$ via the dislocation strain field.⁴ This elastic distortion extends from the dislocation up to the surface, where the effect can be profiled by STM as a function of film thickness. The network of edge dislocations is confined to the interface with no threading component, and is established between 3- and 5-

ML InAs thickness, whereupon the slip dislocation systems become active and dominate the surface morphology thereafter.

In the case of a dislocation slip, a discrete surface step is left behind following motion of a dislocation towards the interface, and its subsequent expansion as the misfit segment increases in length. A slip step, by definition, constitutes a discontinuity in the atomic planes exposed at the surface, and is therefore imaged directly by STM, making this situation distinct from the strain-field-induced relaxation effect which characterized the influence of the set of edge dislocations on the surface. Slip steps can be divided into two classes, depending upon the exact kind of slip system with which they are associated. The first kind are the so-called ‘‘perfect’’ type, denoted $\{111\}\langle 110\rangle$, and produce a surface step equal in height to the (220) plane spacing (~ 2 Å). The other possibility is for a Shockley partial slip system, namely, $\{111\}\langle 112\rangle$, giving rise to a nonintegral step height. The presence of the latter type has been confirmed for InAs/GaAs(110) by high-resolution cross-sectional transmission electron microscopy (TEM), where stacking faults were identified on the relevant slip planes.³ In particular, nonconventional surface displacements caused by the slip of partial dislocations provides the opportunity for atomic reorganization which is peculiar to surfaces which have been disturbed in such a fashion. This surface effect is different from, but analogous to, the reconstruction which is thought to occur at the dislocation core.⁶

Although slip steps have been profiled for

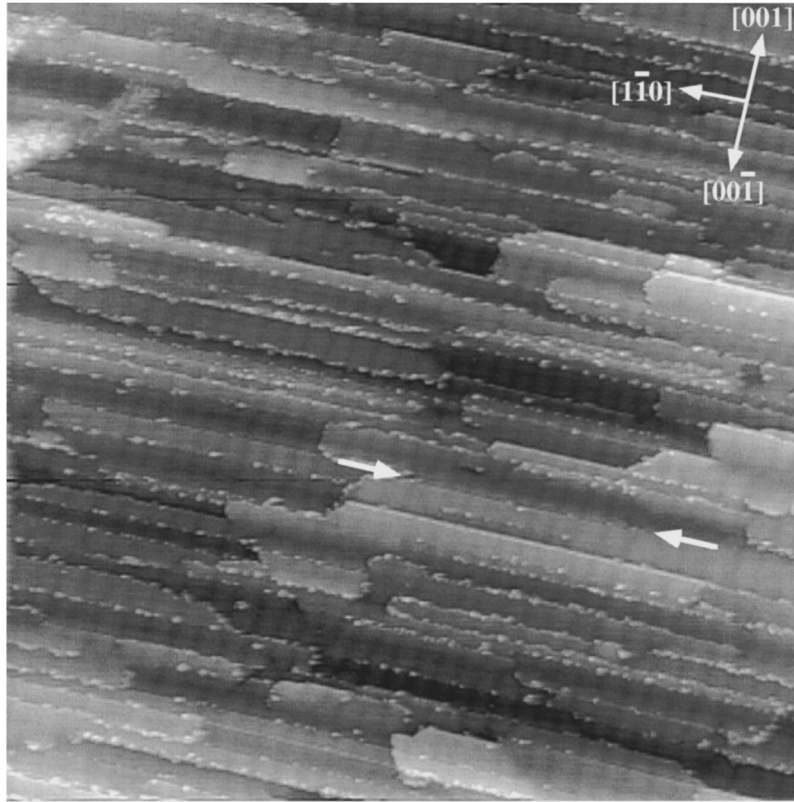


FIG. 1. Filled-states STM image of 10-ML InAs/GaAs(110). Both mechanisms for strain relief are resolved at the surface. The arrows indicate a line feature with no associated change in surface elevation. Image dimensions are $2000 \times 2000 \text{ \AA}^2$.

$\text{Si}_{0.85}\text{Ge}_{0.15}/\text{Si}(001)$ using atomic force microscopy,⁷ the higher lateral resolution afforded by STM allows for a more detailed investigation of the geometric and to some extent electronic structure of isolated slip steps. In this paper, we present STM data for InAs epilayers grown on GaAs(110) by molecular-beam epitaxy (MBE). Different surface atomic configurations due to dislocation activity are observed and rationalized, and the accommodation of these imperfections by continuing epitaxy is also discussed.

II. EXPERIMENT

The samples were prepared and analyzed in a combined MBE-STM facility (DCA, Finland/Omicron GmbH, Germany). Epiready, n^+ -type Si-doped, single-crystal GaAs(110) substrates (American Xtal Technology) were used in this study. They were mounted on molybdenum blocks, and introduced into the vacuum chamber without any further *ex situ* preparation and then thermally cleaned at $\sim 300 \text{ }^\circ\text{C}$. Following removal of the surface oxide layer at $640 \text{ }^\circ\text{C}$, thin (10 ML) homoepitaxial buffer layers of GaAs were grown at a substrate temperature of $520 \text{ }^\circ\text{C}$ and an As/Ga atomic flux ratio of 10. Before heteroepitaxial growth, smooth surfaces were obtained by annealing at $580 \text{ }^\circ\text{C}$.⁸ The indium flux used during the subsequent heteroepitaxial growth of InAs was adjusted to provide a growth rate of approximately 0.13 ML s^{-1} . All data presented in this paper derive from a single InAs layer thickness equivalent to 10 ML ($\sim 20 \text{ \AA}$) grown at a substrate temperature of $420 \text{ }^\circ\text{C}$, although a number of different layer thicknesses and growth conditions were also studied. STM measurements were made

after the samples had been transferred from the growth chamber and allowed to cool to room temperature in the STM chamber. Constant current mode images were obtained for both filled and empty electronic states using sample biases in the range $|V_s| = 2\text{--}4 \text{ V}$, and tunneling currents of $0.05\text{--}0.2 \text{ nA}$.

III. RESULTS AND DISCUSSION

The morphology of the 10-ML InAs/GaAs(110) surface is shown in Fig. 1. A large number of slip steps are present and they are aligned, with little deviation, in the $[110]$ direction. Also visible at this thickness is the buried network of pure edge dislocations, identified as the array of dark ripples in the orthogonal $[001]$ direction.⁴ The linear density of the slip steps is approximately $125 \mu\text{m}^{-1}$, which corresponds to an average separation of nearly 80 \AA . A dislocation slip occurs on the two inclined (111) and $(11\bar{1})$ planes, so that the surface steps can step down in either the $[00\bar{1}]$ or $[001]$ directions, respectively; in addition, there are some linear features over which no change in surface height is obvious (see the arrows in Fig. 1). Clearly, the combination of different slip steps, and their direction of propagation on the surface during growth, makes for a complex morphology which needs to be analyzed in detail.

The range of slip steps present in this heteroepitaxial growth system can be identified from their associated Burgers vectors, which have been determined from previous TEM studies.³ Of the perfect 60° -type dislocations, $\mathbf{b} = a_0/2 [10\bar{1}]$ and $\mathbf{b} = a_0/2 [0\bar{1}1]$ on (111) , and $\mathbf{b} = a_0/2 [101]$ and $\mathbf{b} = a_0/2 [011]$ on $(11\bar{1})$ are observed following slip of the

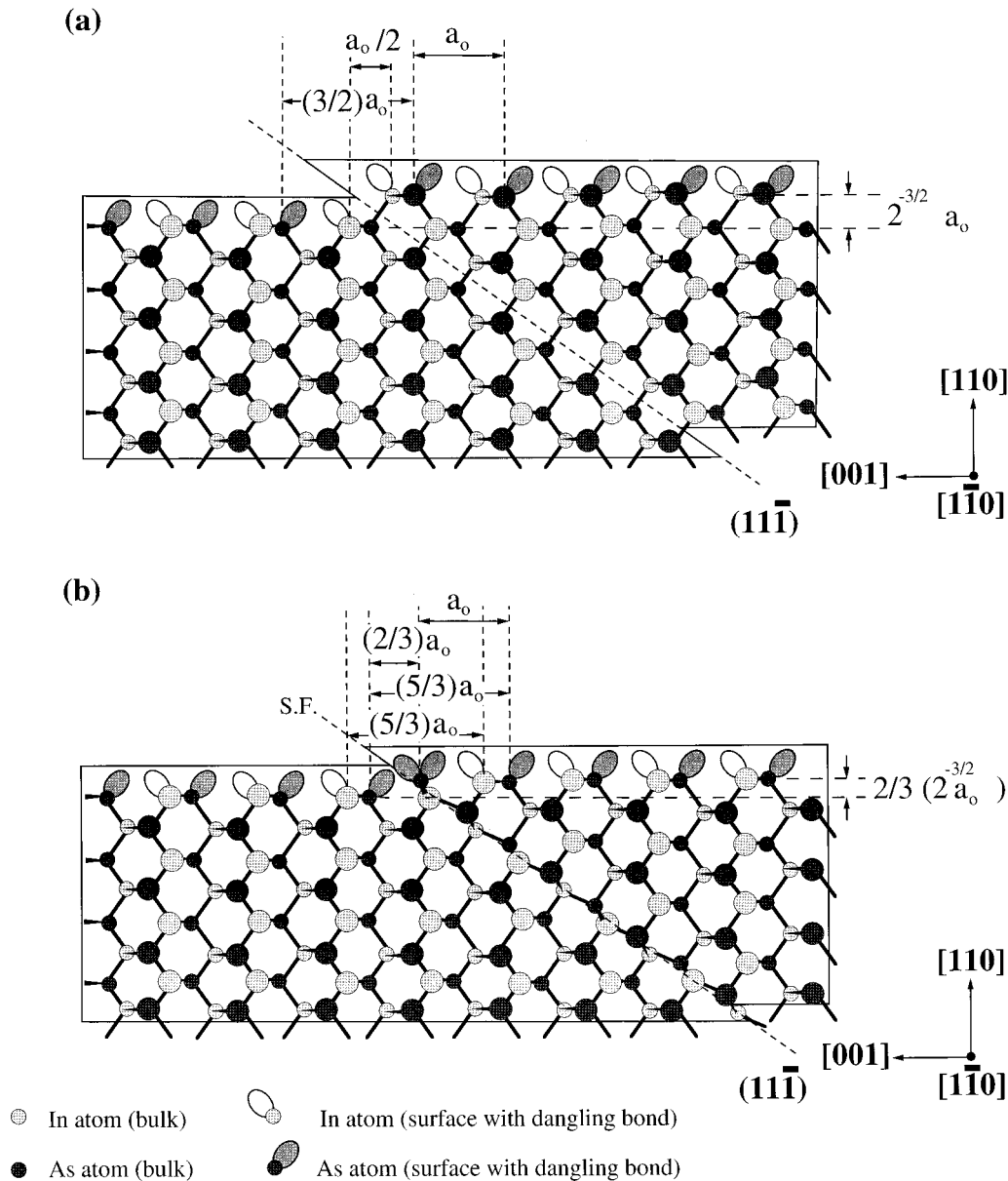


FIG. 2. Schematic diagrams, viewed in the $[1\bar{1}0]$ side projection, showing the structures (before reconstruction) for slip steps formed on the (110) surface after slip on the (111) plane: (a) perfect 60° type, $\mathbf{b} = a_0/2 [101]$ (shuffle set shown); (b) partial 90° type, $\mathbf{b} = a_0/6 [112]$. For slip on the opposite (111) plane, identical structures are formed, but with the atomic species reversed.

“shuffle” kind in between the wider spaced $\{111\}$ planes [Fig. 2(a)]. Both of these give rise to steps 2 \AA in height [equal to the (220) spacing] which are shifted by half the unit cell dimensions parallel to the surface: $\sim 2.8 \text{ \AA}$ ($a_0/2$) along $\langle 001 \rangle$ and $\sim 2 \text{ \AA}$ ($2^{-3/2}a_0$) along $\langle 110 \rangle$.⁹ Slip of perfect dislocations on the glide set is also assumed to be possible. The choice of partial dislocations is subject to some restriction in terms of allowed $\{111\}$ stacking sequences,¹⁰ so that only the 90° set is appropriate here for the relief of compressive strain, i.e., $\mathbf{b} = a_0/6 [11\bar{2}]$ on (111) and $\mathbf{b} = a_0/6 [112]$ on (111). It is accepted that partial dislocation slip is confined within the narrower spaced $\{111\}$ planes and is of the “glide” kind.¹¹ The nominal displacements defining these partial slip steps are $\sim 1.3 \text{ \AA}$ [two-thirds of the (220) spacing] normal to the (110) surface and $\sim 1.9 \text{ \AA}$ ($a_0/3$) parallel to the surface along $\langle 001 \rangle$ [Fig. 2(b)]. There is no displace-

ment in the orthogonal $\langle 110 \rangle$ surface direction for these 90° partial types.

Figure 3 shows two images which were acquired for three individual partial slip steps in both (a) filled- and (b) empty-state imaging modes. The termination of the upper step is evident since it has a component of a right-handed screw dislocation, corresponding to the point at which the threading segment intersects the surface. The steps can all be identified as $\mathbf{b} = a_0/6 [112]$ type, with reference to the 1.3-\AA step height [line profile A in Fig. 3(a)] and the lateral atomic separations along $[001]$ over the step [Fig. 2(b)]. The last row of atoms at the upper edge of each slip step is largely incomplete, with only short strips of material remaining. This is shown most clearly in the filled-state image [Fig. 3(a)]. They are approximately 30 \AA in length, and appear to consist of a series of dumbbell-shaped features (arrow 1). The lobes within each

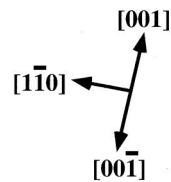
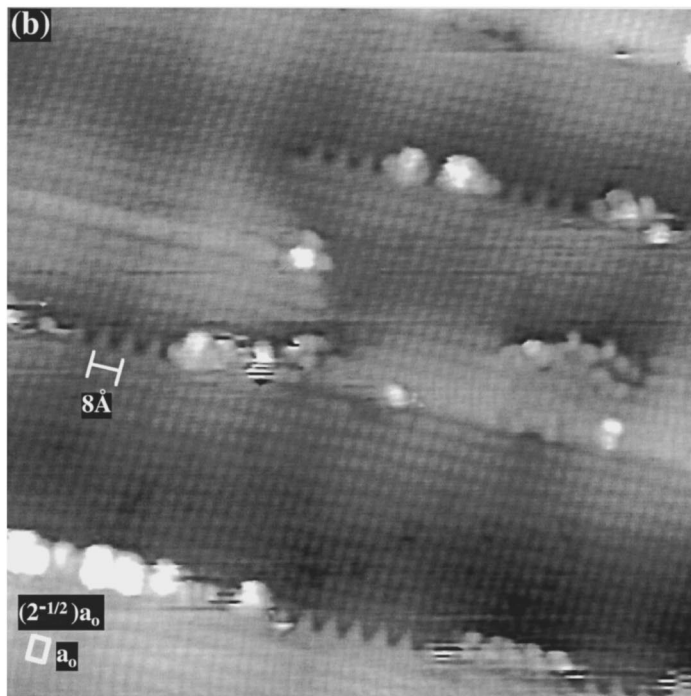
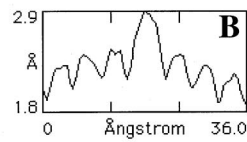
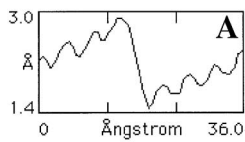
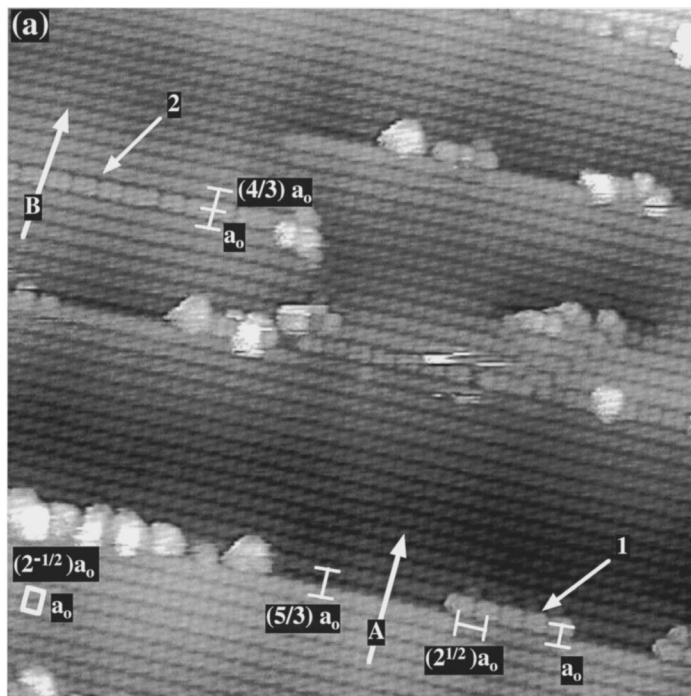


FIG. 3. STM images ($200 \times 200 \text{ \AA}^2$) containing partial slip steps after slip of the kind $\mathbf{b} = a_0/6 [1\bar{1}2]$: (a) Filled-state mode ($V_{\text{sample}} = -2 \text{ V}$); the arrows indicate the position of dimer features (1) at a step edge and (2) within a terrace. (b) Empty-state mode ($V_{\text{sample}} = +2 \text{ V}$) showing triangular step-edge protrusions. The line profiles A and B are shown below (a), and the 1×1 unit-cell dimensions are also shown in the bottom-left corner of each image.

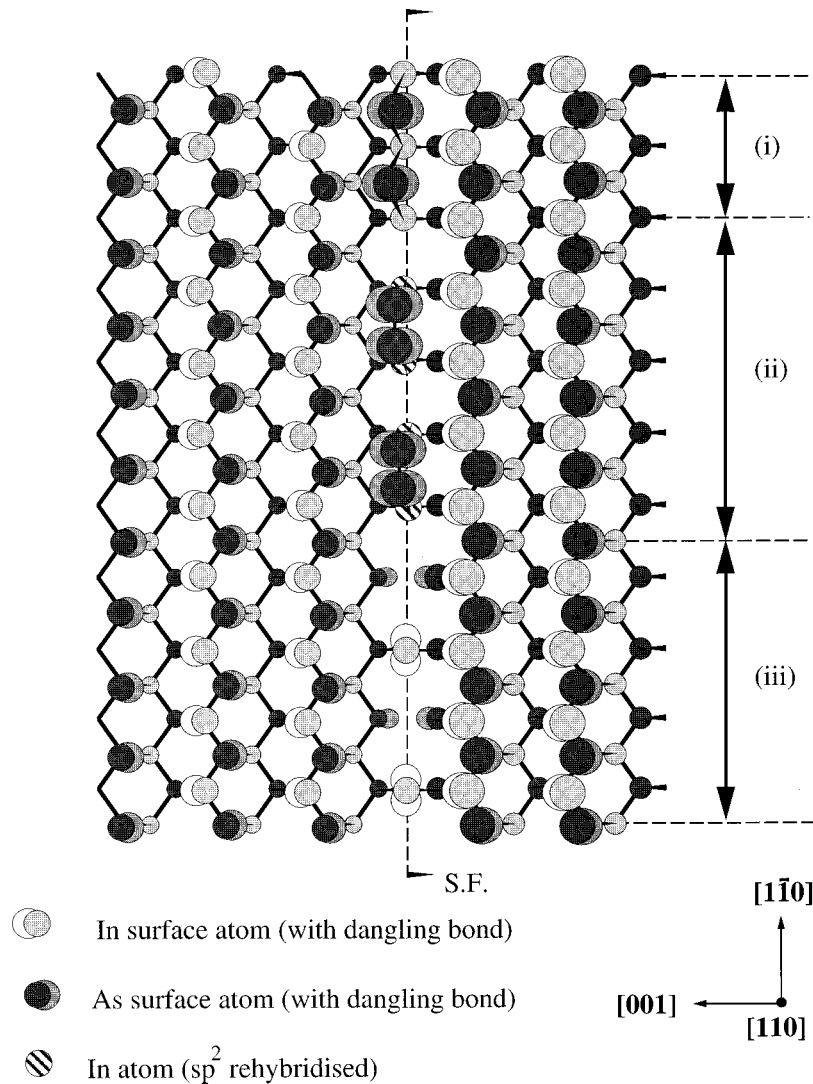


FIG. 4. A schematic diagram corresponding to a $[1\bar{1}0]$ plan view structural model for a 40-Å-long section of slip step. The intersection of the $(11\bar{1})$ stacking fault (S.F.) is along the dashed line, and this is divided into three sections: (i) nominal structure [as in Fig. 2(b)], (ii) dimer model (the cross-hatched indium atoms denote possible rehybridization from sp^3 to sp^2), and (iii) the missing indium autocompensated model.

dumbbell are separated by nearly 3 Å, and the dumbbell periodicity is $\sim 8 \text{ \AA} (2^{1/2}a_0)$, which is exactly twice the atomic period along $[1\bar{1}0]$ [i.e., $(a_0/2^{1/2}) \sim 4 \text{ \AA}$]. The dumbbells thus bear a constant phase relationship with the normal arsenic (or indium) periodicity in the terraces, and it is evident on close inspection that the center of each dumbbell node is aligned with a $[001]$ row of arsenic atoms.

A plan view representation of a proposed structure for these features is given in Fig. 4. The indium atoms at the stacking fault S.F. must undergo a 180° rotation in their sp^3 orbital geometry to constitute the disruption in the stacking sequence. For the row of arsenic atoms at the surface bonded directly to these rotated indium atoms at the position where the stacking fault meets the surface, the possibility arises of local reconstruction involving dimerization [Fig. 4, section (i)]. The observed dumbbell shape is thus consistent with an arsenic-arsenic dimer pair, with a bond length of $\sim 3 \text{ \AA}$, and centered correctly on a row of arsenic atoms [Fig. 4, section (ii)]. It also seems likely that the underlying indium atoms rehybridize to an sp^2 configuration (cross-hatched in Fig. 4)

to relieve some of the strain in the reconstruction, as found in the surface relaxation characteristics of III-V and II-VI cleavage plane surfaces.¹² We note, however, that this proposed reconstruction is neither electronically autocompensated (each As dimer atom is deficient by one electron), nor does it lead to a reduction in the dangling-bond density,¹³ and is derived solely for geometric consistency with the STM image. It should be noted, however, that conventional monolayer steps along $[1\bar{1}0]$, such as those also produced by perfect dislocation slip, are also not autocompensated, and other step directions may also carry a net charge.^{14,15} Furthermore, the failure to satisfy the chemical valency is reasonable, since the dislocation core, where dangling bonds are also exposed, can carry a net electronic charge which may have consequences for electron transport behavior.^{16,17}

The dimers can also be observed in the middle of a terrace, as well as along a slip step edge, as can be seen in the position highlighted in Fig. 3(a) (arrow 2). These linear features are formed on the junction of a slip step of the kind just discussed, and another partial slip step formed through slip

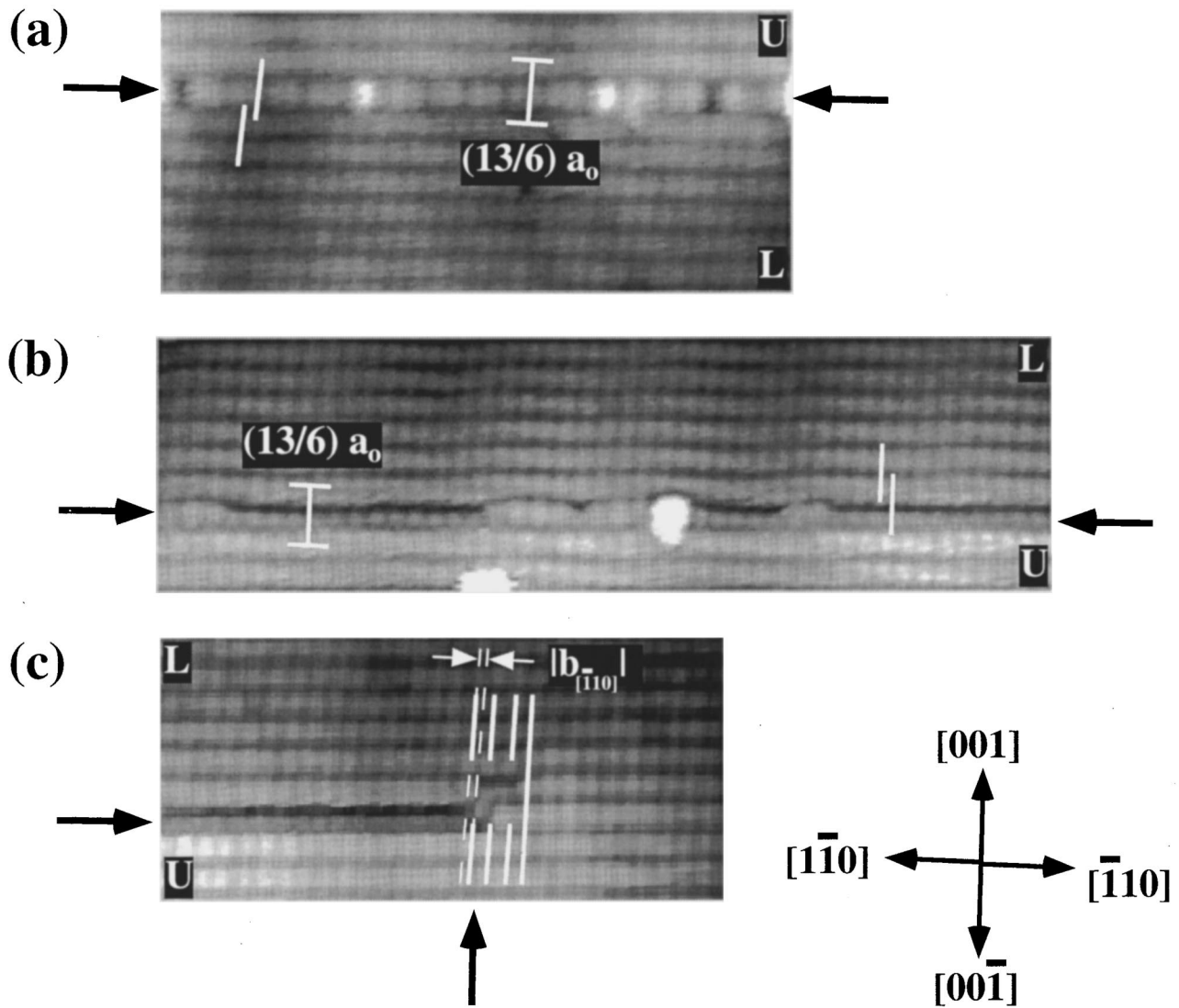


FIG. 5. Filled-state STM images of the two types of junctions formed by the coalescence of perfect and partial steps after slip on the opposing (111) and $(1\bar{1}\bar{1})$ planes. The upper and lower terraces behind the perfect and partial slip steps are labeled U and L , respectively; the width of both junctions are shown as $\frac{13}{6}a_0$; and the relative shift by half the unit cell length in the $[\bar{1}\bar{1}0]$ direction by $(2^{-3/2})a_0$ is highlighted by the pairs of white lines: (a) ($120 \times 50 \text{ \AA}^2$) involving $\mathbf{b} = a_0/2 [10\bar{1}]$ or $\mathbf{b} = a_0/2 [01\bar{1}]$ (perfect) and $\mathbf{b} = a_0/6 [11\bar{2}]$ (partial) steps. (b) ($170 \times 50 \text{ \AA}^2$) involving $\mathbf{b} = a_0/2 [01\bar{1}]$ (perfect) and $\mathbf{b} = a_0/6 [11\bar{2}]$ (partial) steps. (c) ($105 \times 50 \text{ \AA}^2$) same step construction as (b), showing a Burgers circuit to determine the direction and magnitude of the component of the perfect dislocation along the step junction, i.e., $|\mathbf{b}([\bar{1}\bar{1}0])| = 2^{-3/2}a_0$.

on the opposite (111) plane of $\mathbf{b} = a_0/6 [11\bar{2}]$ type. Since both partial slip steps produce the same change in surface height, there is no net difference on their common junction [line profile B in Fig. 3(a)]. There is, however, a slight difference in the separation of the dimers from the adjacent rows of arsenic atoms when measured along $\langle 001 \rangle$. The difference is just 1.9 \AA ($a_0/3$) larger along $[001]$ than along $[00\bar{1}]$, implying that the dimers “belong” to the lower slip step forming the junction. Indeed, images of the opposite $\mathbf{b} = a_0/6 [11\bar{2}]$ slip step, when observed individually, do not involve any such dimer features. The dimers only display short-ranged order due to occasional switches of 180° in the dimerization direction, and may be completely absent for short sections to leave a trough feature. The junction between the same two opposing partial slip steps can also be observed without the row of dimers. In this case, there is a

small disruption in the atomic periodicity measured along $\langle 001 \rangle$ in the form of a single wide $(4/3)a_0$ inter-row spacing for both arsenic and indium species.

As already indicated, the arsenic dimers are only found along parts of the slip step edge and are frequently absent, which leaves the indium atoms at the stacking fault exposed. The consequence of this is seen only in the image taken in the empty-state tunneling mode, where triangular protrusions are observed wherever the dimers are absent from the step edge [Fig. 3(b)]. These features possess the same double ($\sim 8 \text{ \AA}$) periodicity along $[1\bar{1}0]$ as the dimers, but are centered on the $[001]$ -directed rows of indium atoms. The favored structure for this situation is obtained by removing half of the indium atoms on the stacking fault to expose two three coordinated As atoms for every one of the two coordinated indium atoms extracted [Fig. 4, section (iii)]. Charge neutral-

ity can thus be achieved in this case via electron transfer from the remaining In atoms to the As atoms. The observation of these depressed As atoms would require resolution of distances $< 3 \text{ \AA}$ below the primary surface level which is made difficult by the lateral resolution limit of STM ($1\text{--}2 \text{ \AA}$). The surface indium atoms, however, which possess two unoccupied dangling bonds each, are observed in STM when operated in empty-state mode. Their triangular shape is curious, but may correspond to some antibonding electron state produced from a combination of atomic orbitals. An indirect indication that the structure in Fig. 4 (iii) may be accurate is the frequent observation of disordered assemblies of material decorating the slip step edges which could be interpreted as displaced In atoms which cannot desorb at typical growth temperatures.

In Fig. 5, the principle of slip step coalescence, the inevitable result of growth on a surface containing these features, is demonstrated further. In these images, the resolved structures include slip steps due to 60° perfect type dislocations in addition to the partial types already discussed. These 60° slip steps have a readily recognizable trait since the upper (U) and lower (L) sides of the step, being adjacent (220) planes, possess an obvious shift in the positions of the surface atoms by an amount equal to half the surface unit-cell dimensions in both the $[001]$ and $[\bar{1}10]$ directions. There is no such shift on traversing a partial slip step, such as those contained in Fig. 3. This distinction, as well as the height of any remaining step, enables the two slip steps contributing to each junction to be identified. The height difference for both of the steps shown in Figs. 4(a) and 4(b) is $\sim 0.7 \text{ \AA}$ [one-third of the (220) plane spacing], which would result from the junction of a 60° perfect and a 90° partial slip step.¹⁸ Further, the combined width of both junctions along the $[001]$ direction is $13/6a_0$, due to the sum of the $5/3a_0$ partial displacement and the $a_0/2$ shift from the perfect step. The organization of the material within the $13/6a_0$ gap is different, however, in both cases.

The structure of Fig. 5(a) appears initially very similar to that formed from the two partial steps in Fig. 3 [arrow (2)] since a row of dumbbell shaped arsenic dimers is also formed at this junction. The characteristic shift by $2^{-3/2}a_0$ ($\sim 2 \text{ \AA}$) along $[\bar{1}10]$ and the $13/6a_0$ width in $[001]$, however, identify this as the junction of two slip steps associated with the perfect $\mathbf{b} = a_0/2 [\bar{1}01]$ (or $\mathbf{b} = a_0/2 [01\bar{1}]$) and partial $\mathbf{b} = a_0/6 [112]$ dislocations. In fact, the 0.7-\AA -higher terrace is found to be above the junction in the STM image. In contrast, the higher terrace is below the junction which is shown in Fig. 5(b), so that this structure must occur as a result of

coalescence of the other perfect/partial step pair, namely, $\mathbf{b} = a_0/2 [10\bar{1}]$ (or $\mathbf{b} = a_0/2 [011]$) and $\mathbf{b} = a_0/6 [11\bar{2}]$. A recessed $[\bar{1}10]$ row of atoms with an uninterrupted $\sim 4 \text{ \AA}$ ($a_0/2^{1/2}$) periodicity is observed [bounded by arrows in Fig. 4(b)] which is aligned with the arsenic atoms above the junction, but displaced $\sim 2 \text{ \AA}$ [$(2^{-3/2})a_0$] compared to those below. Thus the alignment of the recessed row along $[\bar{1}10]$ associates it with the material lying on or above the stacking fault of the partial dislocation. It is also occasionally displaced vertically by $\sim 0.5 \text{ \AA}$, so that the atoms lie approximately at the same height as the surface level on either side of the junction. The magnitude of this distortion is consistent with a surface relaxation, and may indicate the accommodation of some surface strain at the slip step junction. The screw terminus of the feature in Fig. 5(b) is provided in Fig. 5(c), from which the in-plane $[\bar{1}10]$ component of the Burgers vector of the perfect dislocation can be extracted by completing the appropriate Burgers circuit. Additionally, since the shift parallel to the junction has occurred in the $[\bar{1}10]$ direction (as opposed to $[\bar{1}\bar{1}0]$), the Burgers vector of the perfect dislocation can be unambiguously identified as $\mathbf{b} = a_0/2 [011]$ (as opposed to $\mathbf{b} = a_0/2 [101]$).

IV. CONCLUSIONS

The atomic organization found at surface steps following dislocation slip has been discussed for InAs/GaAs(110) heteroepitaxy. The compressive nature of the epilayer strain, as well as the (110) orientation of the substrate, reduces the possible number of slip steps to six. Two of these are due to partial type dislocations, which produce distinctive surface displacements, enabling the formation of structures unique to the otherwise unreconstructed (110) surface of III-V semiconductors. Structural models have been proposed for these configurations and the possible implications for the electronic character of the step edge are also addressed. The other four steps are linked to the perfect class of dislocations which, besides from the screw termini of each step line, incur entirely conventional surface displacements for a (110) surface step. The interaction between these two types has also been observed as a consequence of the continuation of epitaxial growth after their nucleation.

ACKNOWLEDGMENTS

We would like to thank Dr. A. R. Avery and Dr. X. M. Zhang for many helpful discussions. This work was supported by the EPSRC (U.K.) under Grant Nos. GR/J97540 and GR/K23775.

*Permanent address: Department of Physics, University of Warwick, Coventry, CV4 7AL, U.K.

†Current address: Chartered Semiconductors, Corporate R&D, Thin Film Division, 60 Woodlands Industrial Park D, Street 2, Singapore 738406.

‡FAX: 44(0)171 594 5801. Electronic address: t.jones@ic.ac.uk

¹J. W. Matthews and A. E. Blakeslee, *J. Cryst. Growth* **27**, 118 (1974).

²D. W. Pashley, *Philos. Mag.* **A 67**, 1333 (1993).

³X. Zhang, D. W. Pashley, L. Hart, J. H. Neave, P. N. Fawcett, and B. A. Joyce, *J. Cryst. Growth* **131**, 300 (1993).

⁴J. G. Belk, J. L. Sudijono, X. M. Zhang, J. H. Neave, T. S. Jones, and B. A. Joyce, *Phys. Rev. Lett.* **78**, 475 (1997).

⁵J. G. Belk, J. L. Sudijono, H. Yamaguchi, X. M. Zhang, D. W. Pashley, C. F. McConville, T. S. Jones, and B. A. Joyce, *J. Vac. Sci. Technol. A* **15**, 915 (1997).

⁶P. B. Hirsch, *Mater. Sci. Technol.* **1**, 666 (1985).

⁷M. A. Lutz, R. M. Feenstra, F. K. LeGoues, P. M. Mooney, and J. O. Chu, *Appl. Phys. Lett.* **66**, 724 (1995).

⁸D. M. Holmes, J. G. Belk, J. L. Sudijono, J. H. Neave, T. S. Jones, and B. A. Joyce, *J. Vac. Sci. Technol. A* **14**, 849 (1996); D. M. Holmes, J. G. Belk, J. L. Sudijono, J. H. Neave, T. S.

- Jones, and B. A. Joyce, *Surf. Sci.* **341**, 133 (1995).
- ⁹For simplicity, the lattice parameter for GaAs has been used ($a_0 = 5.65 \text{ \AA}$) in quoting all absolute displacements. The actual lattice parameter will be up to 7% greater than this due to strain relief in the InAs epilayer.
- ¹⁰D. W. Pashley, *J. Cryst. Growth* **162**, 178 (1996).
- ¹¹P. Pirouz and X. J. Ning, *Inst. Phys. Conf. Ser.* **146**, 69 (1995).
- ¹²See, for example, H. Lüth, *Surfaces and Interfaces of Solid Materials*, 3rd ed. (Springer-Verlag, Berlin, 1995), p. 299ff.
- ¹³M. Wassermeier, J. Sudijono, M. D. Johnson, K. T. Leung, B. G. Orr, L. Daerwitz, and K. H. Ploog, *J. Cryst. Growth* **150**, 425 (1995).
- ¹⁴J. M. McCoy and J. P. LaFemina, *Phys. Rev. B* **54**, 14 511 (1996).
- ¹⁵M. Heinrich, C. Domke, Ph. Ebert, and K. Urban, *Phys. Rev. B* **53**, 10 894 (1996).
- ¹⁶F. R. N. Nabarro, *Theory of Crystal Dislocations* (Dover, New York, 1987), p. 641.
- ¹⁷D. B. Holt, *J. Mater. Sci.* **1**, 280 (1966).
- ¹⁸It should be noted that the step height and $[\bar{1}\bar{1}0]$ shift produced by an isolated 30° partial slip step could also generate this step height; however, these dislocations are suitable only for tensile-strained layers; see Ref. 10.